Enhanced diffusiophoresis in dead-end pores with time-dependent boundary solute concentration

Robben E. Migacz ⬤, Morgan Castleberry, and Jesse T. Ault ⬤*
Center for Fluid Mechanics, School of Engineering, Brown University,
Providence, Rhode Island 02912, USA

The dead-end pore is a geometry common to studies of diffusiophoresis. In most works on diffusiophoresis in dead-end pores, the solute concentration at the pore inlet is quickly changed between two extreme values, yielding a steplike change in solute concentration. We explore—noting diffusiophoresis is inherently nonlinear and other boundary conditions are largely unexplored—the influence of a time-variable boundary solute concentration. We first define metrics for the efficiency of diffusiophoretic injection and withdrawal and characterize the steplike boundary condition. We then introduce a linear change in solute concentration over a variable timescale and comment on changes in efficiency. We find particle migration becomes linear in the limit of slow transitions relative to the timescale for solute diffusion and define an asymptotic efficiency. We further characterize oscillatory changes in the boundary solute concentration and the implications of the oscillation frequency, from slow (yielding linear particle migration) to fast (yielding nonlinear paricle migration) oscillation. The particle dynamics are distinct and can be tuned by adjusting the timescale for oscillation. Our findings are relevant to processes both in the laboratory, where they could inform the choice of timescale or oscillation frequency for changes in solute concentration, and in nature, where various events cause solute concentrations to change over distinct and disparate timescales.

I. INTRODUCTION

The dead-end pore is a geometry commonly considered in studies of diffusiophoresis, the migration of particles in the presence of a solute concentration gradient. The dead-end pore, on account of limited convection except in the near-inlet region, allows researchers to focus on diffusion and electrokinetic transport phenomena as drivers of solute and particle migration. In such a geometry, the difference between the timescales for the diffusion of the solute and particles can be significant, depending on the species involved. Shin *et al.* [1] consider, for example, polystyrene latex particles between 0.06 and 1.01 μm in diameter in gradients of NaCl; the diffusion timescales of the particles and the solute differ by factors between 190 and 3400, depending on the particle size. In a practical setting, such as the 400 μm-long channel used by Shin *et al.* [1], this is the difference between solute diffusing over a timescale measured in minutes and micrometer-scale particles diffusing over a timescale measured in days. In this context, diffusiophoresis—which imparts a particle velocity proportional to the gradient of the logarithm of the solute concentration [2]—emerges as a practical mechanism for enhancing the rate of particle transport to or from dead-end pores.

Diffusiophoresis in dead-end pores has numerous potential applications. First, it can be used to characterize the size and zeta potential of particles, as demonstrated in several works by Shin

---

*jesse_ault@brown.edu

(a) Step boundary, typical of past experiments

(b) Repeated step boundary

(c) Arbitrary boundary

Distinct flow rates

Immiscible fluid   Pore
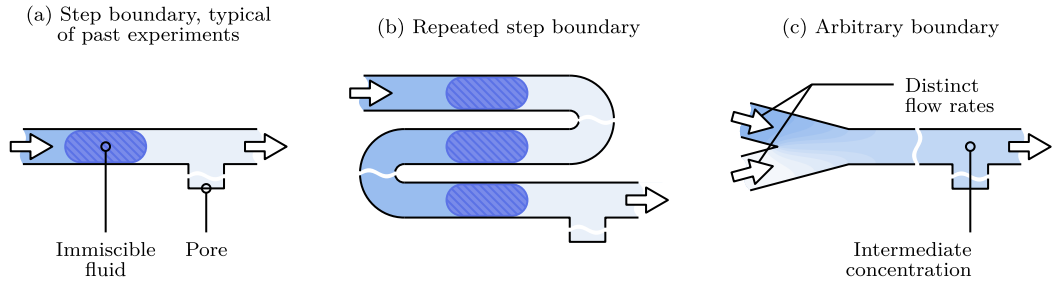
Intermediate concentration

FIG. 1. Strategies for changing the solute concentration at the inlet of a dead-end pore. The step boundary, shown in (a), is typical of experiments involving diffusiophoresis in dead-end pores. A repeated step boundary condition, depicted in (b), could be used to change the concentration at the boundary between extreme values multiple times. The Y-channel configuration shown in (c) could be used to obtain an arbitrary concentration between the extreme concentrations by modulating the flow rate of each inlet. Configurations (b) and (c) could yield an oscillatory solute concentration at the pore inlet, and configuration (c) could be used to change the concentration arbitrarily with relatively slow and smooth transitions between extreme concentrations.

et al. [1,3]. This is particularly relevant where conventional methods of particle characterization are impractical because of issues of cost or availability. Unlike electrophoresis, diffusiophoresis does not require an external field to drive particle motion [4] and could be applied to low-cost or mobile devices. Second, diffusiophoresis in dead-end pores is likely relevant to geological processes and related industrial applications, such as enhanced oil recovery [5]. Third, it may be relevant to numerous biological processes [5,6]; Vrhovec Hartman *et al.* [6] propose, for instance, that it may be an important consideration for cell-culturing microchambers. Peter *et al.* [7] demonstrate that diffusiophoresis is significant even for individual proteins and Wanunu *et al.* [8] suggest that solute gradient-driven migration of DNA in nanopores may be useful for the analysis of biological samples. The number and variety of potential applications has driven considerable research interest in diffusiophoresis in dead-end pores in recent years.

Researchers commonly produce a solute concentration gradient by quickly switching the concentration of a reservoir in contact with the entrance of the pore [1,3,7,9–17]. We show a typical experimental configuration in Fig. 1(a). In such a configuration, researchers use an immiscible fluid to separate solutions with distinct solute concentrations. Flow in the channel switches the concentration at the pore entrance over a very short time, resulting in a steplike change in boundary concentration. The resulting sharp solute concentration gradient causes particle migration through diffusiophoresis.

Several researchers have considered boundary conditions other than a step for the solute concentration. Shin *et al.* [1] comment, for example, on a system with a gradual change in solute concentration (cf. Fig. 1), but the work focuses on the step boundary condition. Kar *et al.* [5] and Chiang and Velegol [18] use a different experimental configuration with a small capillary test section inserted into a larger capillary serving as a reservoir. Such a configuration may yield a slower change in boundary solute concentration relative to other researchers' experiments, for which flow past the pore maintains a consistent concentration at the inlet, but the boundary condition is not the focus of the works. In a distinct geometry, Palacci *et al.* [19] demonstrate that oscillation in solute concentration at the boundaries of a cell containing particles can lead to focusing "limited [only] by ... diffusion of the colloids." They show that the nonlinear relationship between diffusiophoretic velocity and solute concentration can be applied practically in microfluidic devices, though they do not examine the potential utility in dead-end pores.

The potential utility of solute boundary conditions beyond the step in dead-end pore geometries is the basis of our present work. We examine whether alternatives to the step solute concentration boundary, such as a slow transition between extreme concentrations, can be more effective at

yielding particle migration into or out of the pore. We also consider whether oscillatory changes in boundary solute concentration may be of interest to researchers. We propose potential mechanisms for changing the solute concentration to exploit the nonlinearity of diffusiophoresis—the diffusiophoretic velocity is proportional to the gradient of the logarithm of solute concentration—in Figs. 1(b) and 1(c). In Fig. 1(b), we extend the configuration in Fig. 1(a) by repeatedly switching between two extreme concentrations. In Fig. 1(c), we show how it is possible to achieve smooth transitions between solute concentrations with a Y-channel with independent inlets. In such a system, the concentration at the entrance of the pore is approximately equal to the flow rate-averaged concentration of the inlets, provided there is sufficient time for the solute to diffuse prior to flowing past the pore. The configuration in Fig. 1(c) allows for a relatively slow transition between concentrations, in stark contrast to the steplike behavior in Fig. 1(a) and 1(b). The setup is similar to that used in experiments by Palacci *et al.* [19].

As a result of the nonlinear nature of diffusiophoresis (for which diffusiophoretic velocity depends nonlinearly on solute concentration), it is often necessary to perform numerical experiments to draw conclusions about particle dynamics. We use such experiments to build on a sequence of problems of increasing complexity rather than defining a single problem. To this end, we address several closely related questions—both theoretically and numerically—in this work. We consider, in sequence, the questions

(Q1) How can we define the efficiency of diffusiophoresis in a dead-end pore?

(Q2) What is the efficiency of diffusiophoretic particle migration with a step boundary condition?

(Q3) How does the step boundary condition compare to other options, such as a slow change in concentration? Is there a better alternative in practical settings?

(Q4) Can the nonlinearity inherent to diffusiophoresis be exploited to increase the rate—or change the direction—of particle migration with oscillations in the boundary condition?

We address Q1 in Sec. III by defining the efficiency in terms of a length scale. We then turn to the step boundary condition and describe the associated solute and particle dynamics in Sec. V to answer Q2 before examining the role of time-dependent solute boundary conditions in Sec. VI to address Q3. Finally, we study oscillatory boundary conditions in Sec. VII to address Q4 before discussing our findings in Sec. VIII.

We use the nomenclature of Ault *et al.* [15] throughout, with "injection" referring to particle migration into the pore and "withdrawal" referring to particle migration out of the pore. The direction of particle migration is an important distinction, as Q4 suggests, because particles can move either up or down the solute concentration gradient depending on the signs of the gradient and the diffusiophoretic mobility [20].

II. PROBLEM DESCRIPTION

We consider a straight, dead-end pore of length ℓ. To simplify our analyses, we assume that the pore is one dimensional and that it contains quiescent fluid with a dimensionless solute concentration c and particle concentration n. We neglect particle diffusion by assuming it occurs over a long timescale relative to the diffusive timescale of the solute, $\ell^2/\mathcal{D}$, where $\mathcal{D}$ is the solute diffusion coefficient. We further assume that diffusioosmotic flow at the walls of the pore can be neglected and that the diffusiophoretic mobility $\mathcal{M}$ is constant. Initially, we impose a uniform solute concentration of 1 throughout the pore; we use β to denote the dimensionless solute concentration at the pore inlet at the end of the process. We nondimensionalize position with ℓ and time with $\ell^2/\mathcal{D}$. In this simplified system, the dimensionless governing equation for the solute concentration profile is the diffusion equation

$$\frac{\partial c}{\partial t} = \frac{\partial^2 c}{\partial x^2}, \tag{1}$$
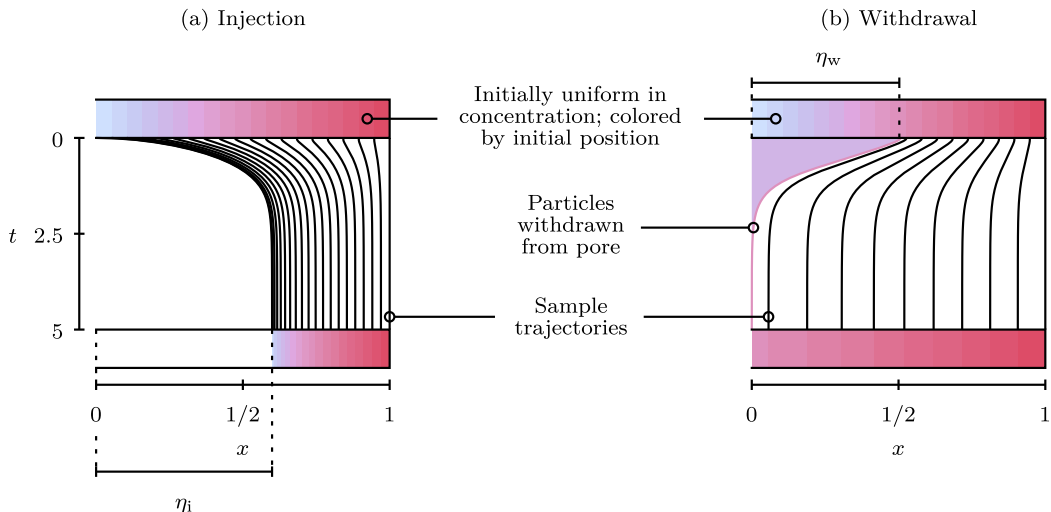
FIG. 2. Definition of injection and withdrawal efficiency values for particle transport in a dead-end pore with a monotonic change in solute concentration at the boundary. We impose a uniform particle concentration in the pore at $t = 0$. The distance the leading particle in (a) travels is the injection efficiency. The initial position of the particle that approaches $x = 0$ for large t in (b) is the withdrawal efficiency. We produced the images in (a) and (b) with a step boundary condition with $\beta = 1/10$ and either (a) $\mathcal{M}/\mathcal{D} = 1/4$ or (b) $\mathcal{M}/\mathcal{D} = -1/4$.

where c is the solute concentration, t is time, and x is position, with boundary conditions

$$c(x = 0, t) = f(t) \qquad \text{and} \tag{2}$$

$$\frac{\partial c}{\partial x}(x = 1, t) = 0, \tag{3}$$

subject to the initial condition

$$c(x, t = 0) = 1. \tag{4}$$

Equations (2) and (3) describe, respectively, the known concentration at the inlet, $f(t)$, and the no-flux condition [21] at the end of the pore.

The particles within the pore undergo diffusiophoresis and migrate in the solute concentration gradient that results from a change in concentration at the boundary. The diffusiophoretic velocity of particles is

$$u = \frac{\mathcal{M}}{\mathcal{D}} \frac{d \ln c}{dx}. \tag{5}$$

Rather than modeling a continuous particle field, we consider individual particles. This reduces the computational effort required to model particle migration; we elaborate on our solution procedure in Sec. IV. Our model for the system consists of Eqs. (1)–(5), with a time-dependent boundary solute concentration $f(t)$.

III. DEFINITION OF EFFICIENCY

To comment on various injection and withdrawal processes, we first require a common language for quantifying performance. We depict injection and withdrawal processes in Figs. 2(a) and 2(b), respectively. The colors in the figure indicate the initial positions of particles, which are initially uniform in concentration. In Fig. 2(a), the particles are compressed nonuniformly, which is a phenomenon that has been observed experimentally [1]. In Fig. 2(b), the particles are drawn toward

the entrance of the pore and some are withdrawn. In the case of a withdrawal process, an apparent choice for efficiency is the ratio of the number of particles withdrawn from the pore to the number of particles present at the start of the process. In cases where the initial particle concentration in the pore is uniform and the change in the solute concentration at $x = 0$, $f(t)$, is monotonic, this can be written instead as a ratio of lengths; the length over which particles are withdrawn relative to the length of the pore is the withdrawal efficiency, η_w, shown in Fig. 2(b).

Casting the injection efficiency as a ratio of lengths is a natural choice, given the prior definition for withdrawal efficiency. We define a process with an injection efficiency of $\eta_i = 1$ as a process during which a particle moves from $x = 0$ to 1, which corresponds to the compression of all particles initially in the pore to the boundary at its end. The injection efficiency is depicted in Fig. 2(a).

Such definitions of efficiency in terms of the length of the pore are applicable only when the boundary solute concentration changes monotonically. Otherwise, the number of particles in the pore is dependent on the particle concentration in the channel, and nonuniformity in the concentration field—a variable density—results in a decoupling of length scales from the number of particles. Indeed, the definition of withdrawal efficiency in terms of a length scale requires an initially uniform particle concentration throughout the pore. Alternative definitions are required for cases where the solute concentration at the pore inlet changes nonmonotonically or the initial particle concentration is nonuniform. Further, we note that the definitions do not account for the possible presence of particles in the channel to which the pore is attached; with our definition, for example, the injection efficiency is not affected by particles that are initially present in the channel and are drawn into the pore during the injection process. Regardless of such limitations, however, the definitions of efficiency address Q1 and allow us to compare the performance of processes with distinct solute concentration boundary conditions.

IV. APPROXIMATE SOLUTIONS AND SIMULATIONS

We now address our strategy for calculating the efficiency of injection and withdrawal processes. The solution to the governing equation for the solute concentration profile, Eqs. (1)–(4), is

$$c(x,t) = f(t) - 4 \sum_{a=1}^{\infty} \sin\left[\frac{\pi x}{2}(2a-1)\right] \int_{t_0}^{t} db \, \frac{\exp\left[-\frac{\pi^2(2a-1)^2(t-b)}{4}\right]f'(b)}{\pi(2a-1)}, \tag{6}$$

which includes both spatial variation and temporal decay. Notably, the integrand contains the first derivative of the function $f(t)$ with respect to time. Simplifications are possible in a number of cases; of particular interest are those where the boundary function is a step, a linear function, or a piecewise step or piecewise linear function, which we explore in Appendix. We provide a solution for the solute concentration with a step boundary condition and an approximate solution for an arbitrary piecewise linear function.

We perform numerical simulations to calculate particle trajectories. We use a method with first-order accuracy in time and ensure convergence dynamically by repeating calculations with higher temporal resolution and additional terms in partial sums until the relative error in the target variable (typically the efficiency of the injection or withdrawal process) falls below a threshold given where specific results are mentioned. We include a segment where $f(t)$ is maintained at a constant value for at least five time units following any change in the boundary condition; this allows the solute concentration—and, in turn, the coupled positions of particles—to stabilize (see sample trajectories in Fig. 2, which show that the change in particle position over time decays significantly over this timescale). The diffusion-driven reduction in solute concentration gradient over this time yields a corresponding decay in diffusiophoretic velocity, and particles approach a stable position.

Some of the potential issues with numerical simulations of particles, such as steep gradients in concentration at $x = 0$, can be mitigated by following a particle front. In any extraction or withdrawal process, we can consider a single particle path as a boundary for all other particles. It is

not possible for particle paths to intersect when the only transport mechanism is diffusiophoresis, inertia is negligible, and the particles start at different positions; any particle approaching another would experience a comparable solute concentration magnitude and gradient and, consequently, attain a comparable velocity. This property can greatly simplify calculations of efficiency, provided the initial concentration of particles in the pore is uniform, as stated in Sec. III. Instead of computing the particle concentration field, we can follow the path of a single particle. For injection processes, we initialize this particle at $x(t = 0) = 0$ and follow it forward in time. In this case, any particles at $x > 0$ are also injected deeper into the pore, but their positions and concentrations are not relevant to the calculation of efficiency. For withdrawal processes, we instead initialize the particle at $x = 0$ at the end of the process and integrate its velocity backward in time to determine its position x_0 at $t = 0$. In this case, any particles initially at a position $x < x_0$ are withdrawn from the pore; with a uniform initial particle concentration, the length scale x_0 is proportional to the fraction of particles withdrawn.

We use approximations of analytical solutions for solute concentration, given in Appendix, in simulations. This has several distinct advantages over numerical simulation for both solute and particles. The first advantage is reduced memory usage when calculating withdrawal efficiency. The diffusion equation is time irreversible—it is impossible to move from a more diffuse state to a less diffuse state without prior knowledge of the state of the system at the earlier time— and, to calculate particle trajectories backward in time, it would be necessary to store the solute concentration field in memory for all points in time and space. With an approximate analytical solution, however, we compute concentration locally in both time and space; we need only find the solute concentration gradient at the position of the particle, rather than throughout the pore, to compute the diffusiophoretic velocity. Finally, this local evaluation also means that interpolation of the solute concentration and solute concentration gradient to the particle position in space and time (which would be necessary if the solute concentration were computed at discrete points) is not required.

V. STEP BOUNDARY CONDITION

Given the significance of the step boundary condition in the literature, we first quantify the efficiency of injection and withdrawal processes with steplike changes in the boundary solute concentration. In doing so, we address Q2. The physical parameters relevant to a process with a step change in boundary solute concentration are the dimensionless diffusiophoretic mobility, $\mathcal{M}/\mathcal{D}$, and the dimensionless final solute concentration, β.

We characterize the efficiency of injection and withdrawal processes over a range of values $\mathcal{M}/\mathcal{D}$ and β in Fig. 3, which shows injection processes in Fig. 3(a) and withdrawal processes in Fig. 3(b). Intuitively, the efficiency of each process increases as the magnitude of $\mathcal{M}/\mathcal{D}$ increases and as the contrast between initial and final solute concentrations increases. Notably, however, the nonlinearity of diffusiophoresis results in a distinct efficiency for each process, even where the ratios of final to initial solute concentration and the magnitudes of the dimensionless diffusiophoretic mobility values are equivalent. The processes with $\beta < 1$ have a higher efficiency than those with $\beta > 1$, all else being equal; this reflects the dependence of the diffusiophoretic velocity on the magnitude of the solute concentration.

VI. TIME-VARYING SOLUTE CONCENTRATION BOUNDARY CONDITIONS

We now turn to cases where the concentration at the boundary of the pore changes continuously over time to begin to address Q3. Physically, this is consistent with the experimental configuration shown in Fig. 1(c), where the flow rates of independent inlets with distinct solute concentrations can be adjusted to attain an intermediate concentration at the pore inlet.

Having considered the step boundary condition in Sec. V, we look to the other extreme, where the concentration at the entrance of the pore changes very slowly relative to the timescale for the

Contours of injection or withdrawal efficiency
with a step boundary condition

(a) Injection   (b) Withdrawal

Contours are
given in increments
of 10 %

Contours of
10, 50, and 90 %
have labels

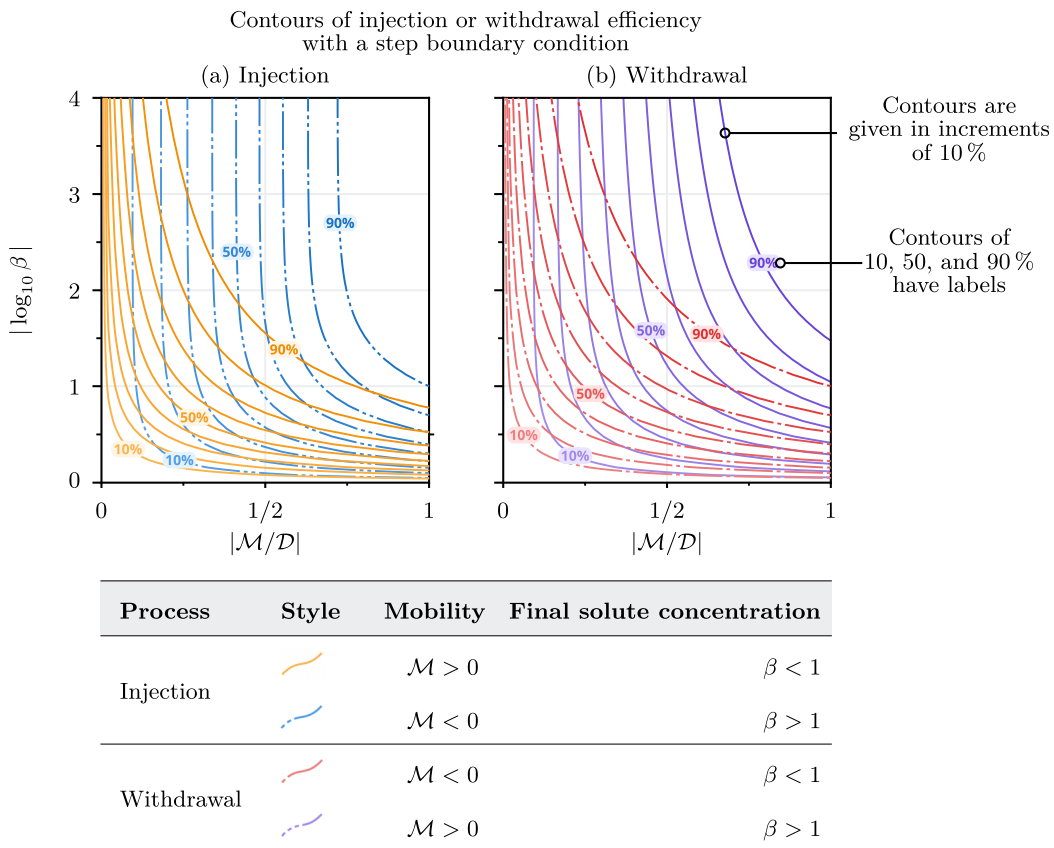| Process	Style	Mobility	Final solute concentration
Injection		$\mathcal{M} > 0$	$\beta < 1$
		$\mathcal{M} < 0$	$\beta > 1$
Withdrawal		$\mathcal{M} < 0$	$\beta < 1$
		$\mathcal{M} > 0$	$\beta > 1$

FIG. 3. Contours of (a) injection and (b) withdrawal efficiency associated with step boundary conditions for a variety of values $\mathcal{M}/\mathcal{D}$ and β. Processes with $\beta < 1$ have a higher efficiency than processes with $\beta > 1$. In general, the efficiency increases as the magnitude of the diffusiophoretic mobility and the difference between final and initial solute concentrations increase. Efficiency values have converged to within 0.0001 %.

diffusion of solute. For a linear transition between solute concentrations occurring over a long time, we obtain a simple analytical expression for the change in the position of a particle. We consider a boundary $f(t) = \phi + mt$ with $m \ll 1$, where the concentration at the boundary transitions linearly to β over a long time. Notably, we have set the initial solute concentration as ϕ instead of 1 [this is a departure from Eq. (4)] so we can consider consecutive processes later; in cases where the solute concentration is changing monotonically, $\phi = 1$. For large t, the solution for a linear boundary condition given in Eq. (A10) becomes
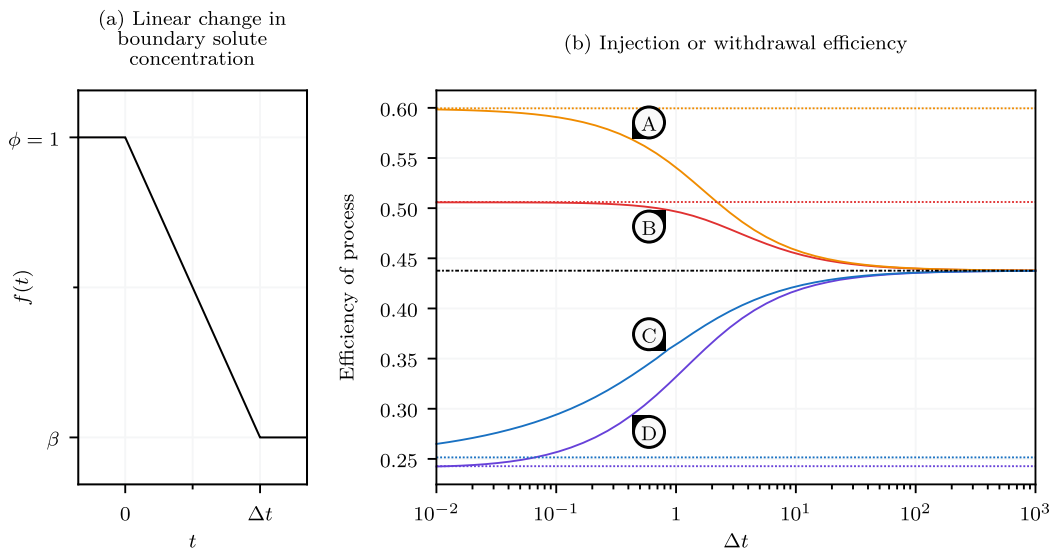
$$\frac{1}{c}\frac{\partial c}{\partial x} = \frac{m(x-1)}{\phi + mt + m(x^2/2 - x)}. \tag{7}$$

To first order in m, this is $m(x-1)/(\phi + mt)$. The diffusiophoretic velocity of a particle is then

$$\frac{dx_p}{dt} = \frac{\mathcal{M}}{\mathcal{D}}\frac{m(x_p - 1)}{\phi + mt}, \tag{8}$$

which we solve to find

$$x_p(x_0) = 1 + \left(\frac{\beta}{\phi}\right)^{\mathcal{M}/\mathcal{D}}(x_0 - 1) \tag{9}$$

(a) Linear change in boundary solute concentration

(b) Injection or withdrawal efficiency

Marker		Process	Ratio of mobility to diffusivity	Final solute concentration
A		Injection	$\mathcal{M}/\mathcal{D} = 1/4$	$\beta = 1/10$
B		Withdrawal	$\mathcal{M}/\mathcal{D} = -1/4$	$\beta = 1/10$
C		Injection	$\mathcal{M}/\mathcal{D} = -1/4$	$\beta = 10$
D		Withdrawal	$\mathcal{M}/\mathcal{D} = 1/4$	$\beta = 10$

Dashed lines indicate efficiency with $\Delta t = 0$ (a step boundary condition)
Dash-dotted line indicates slow-transition asymptote (Eq. 9)

FIG. 4. Example of injection and withdrawal efficiencies for a linear change in solute concentration occurring over time Δt. For this example, we consider $\phi = 1$. We calculate efficiency numerically by performing repeated simulations with smaller time steps and additional terms in truncated approximations of sums until the result has converged to within 0.001% relative error. When the transition time is large relative to the timescale for solute diffusion, the process efficiency approaches the asymptote given in Eq. (9). Notably, the slow-transition efficiency does not change with $\beta \mapsto 1/\beta$ or $\mathcal{M}/\mathcal{D} \mapsto -\mathcal{M}/\mathcal{D}$. Efficiency decreases with increasing Δt if the boundary concentration decreases. Similarly, efficiency increases with increasing Δt if the boundary concentration increases. Colors are consistent with those used in Fig. 3.

at the end of the process, where x_0 is the initial position of the particle. This provides an asymptote for particle migration when the solute concentration at the entrance of the pore changes monotonically and slowly relative to the solute diffusion timescale. The efficiency of injection or withdrawal with a slow change in concentration is then

$$\eta = 1 - \left(\frac{\beta}{\phi}\right)^{\Psi\mathcal{M}/\mathcal{D}}, \tag{10}$$

where $\Psi = 1$ for an injection process and $\Psi = -1$ for a withdrawal process.

Equations (9) and (10) have several interesting properties that we explore with an example in Fig. 4. In our example, we set $\mathcal{M}/\mathcal{D} = \pm 1/4$ and $\log_{10} \beta = \pm 1$ and vary the timescale for the transition in solute concentration, as shown in Fig. 4(a). First, we note that a process with $\beta < \phi$, such as A or B in Fig. 4(b), has a higher efficiency than a process with $\beta > \phi$, such as C or D. This

is an intuitive result; the diffusiophoretic velocity decreases with increasing solute concentration, so increasing the value of the concentration at the boundary has the effect of slowing particles near the pore entrance. This is true of both injection and withdrawal processes. The second property of note is that the efficiency decreases with an increasing transition time Δt between extreme solute concentrations if $\beta < \phi$. The reverse is true for cases where the solute concentration increases: If $\beta > \phi$, then the process efficiency increases with increasing Δt. This result is consistent with those given by Shin *et al.* [1] (cf. Fig. 1), who note reduced particle transport relative to a step with a slow transition in boundary solute concentration when $\beta < \phi$. In response to Q3, then, the step condition yields a higher efficiency when the concentration at the boundary decreases, but slower transitions yield a higher efficiency if the concentration at the boundary increases. Finally, we note that each process approaches the slow-transition asymptote described by Eq. (9) in the limit $\Delta t \to \infty$. This is true of both injection and withdrawal processes, and it holds regardless of the signs of $\mathcal{M}/\mathcal{D}$ and $\log \beta$. The contours shown in Fig. 3 overlap and become symmetric about $\mathcal{M}/\mathcal{D} = 0$ as $\Delta t \to 0$. This has implications for systems with slowly oscillating boundary solute concentrations, which we explore further in Sec. VII A.

VII. OSCILLATORY BOUNDARY CONDITIONS

The nature of diffusiophoresis as an inherently nonlinear process suggests it may be possible to switch the solute concentration at the pore entrance repeatedly to obtain a net benefit to either injection or withdrawal efficiency. Until now, we have only considered cases where the solute concentration changes monotonically. We now relax that requirement and allow the solute concentration at the boundary to oscillate over time, resulting in both particle injection and withdrawal. In doing so, we extend our understanding of Q3 and begin to address Q4.

Notably, with oscillatory boundary conditions, the injection or withdrawal efficiency becomes more difficult to define, as we comment in Sec. III. The concentration of particles *outside* the pore is an important consideration. However, for the sake of argument, we continue using the definitions of efficiency in terms of length and qualify our results where appropriate.

A. Slow oscillation

We first introduce slow (relative to the solute diffusion timescale) oscillation in the solute concentration at $x = 0$. We expect, based on the apparent linearity of diffusiophoresis in dead-end pores with slow changes in the boundary concentration (see Sec. VI), that any particles that remain in the pore over half of one cycle return to their original position at the end of the cycle. We show how the net effect of cyclic diffusiophoresis diminishes as the timescale of injection and withdrawal processes becomes large relative to the solute diffusion timescale in Fig. 5. We impose a sinusoidal boundary solute concentration with a period of 2τ and a magnitude between $\beta = 1/10$ and 1, as shown in Fig. 5(a). When $\tau = 1$ and the period is comparable to the diffusion time for the solute, shown in Figs. 5(b) and 5(c), there is a preferred direction for particle migration caused by asymmetry in $d \ln c/dx$ about the vertical line $t = n\tau$ for $n = 0, 1, 2, \ldots$. The cause of the asymmetry is the time required for the solute to diffuse. When the cycle occurs rapidly relative to solute diffusion, the history of the concentration in the pore has a significant effect on the concentration at a given time: There is a diffusive analog to inertia. As τ increases, as shown in Figs. 5(c), 5(d) 5(f), and 5(g), $d \ln c/dx$ approaches a configuration that is antisymmetric about the vertical line; the diffusion of solute occurs very rapidly relative to the timescale of the process, and the effect of the diffusive inertia becomes less pronounced. At large values of τ, then, any diffusiophoretic migration a particle undergoes during one-half of the cycle is reversed before the start of the next cycle (provided the particle is not withdrawn; conceptually, this is similar to reversibility in flows at low Reynolds number, where inertia is also negligible).

Notably, the linearity of diffusiophoresis for slow injection and withdrawal processes does not imply that the net efficiency is zero. Particles can still be drawn out of or into the pore, depending
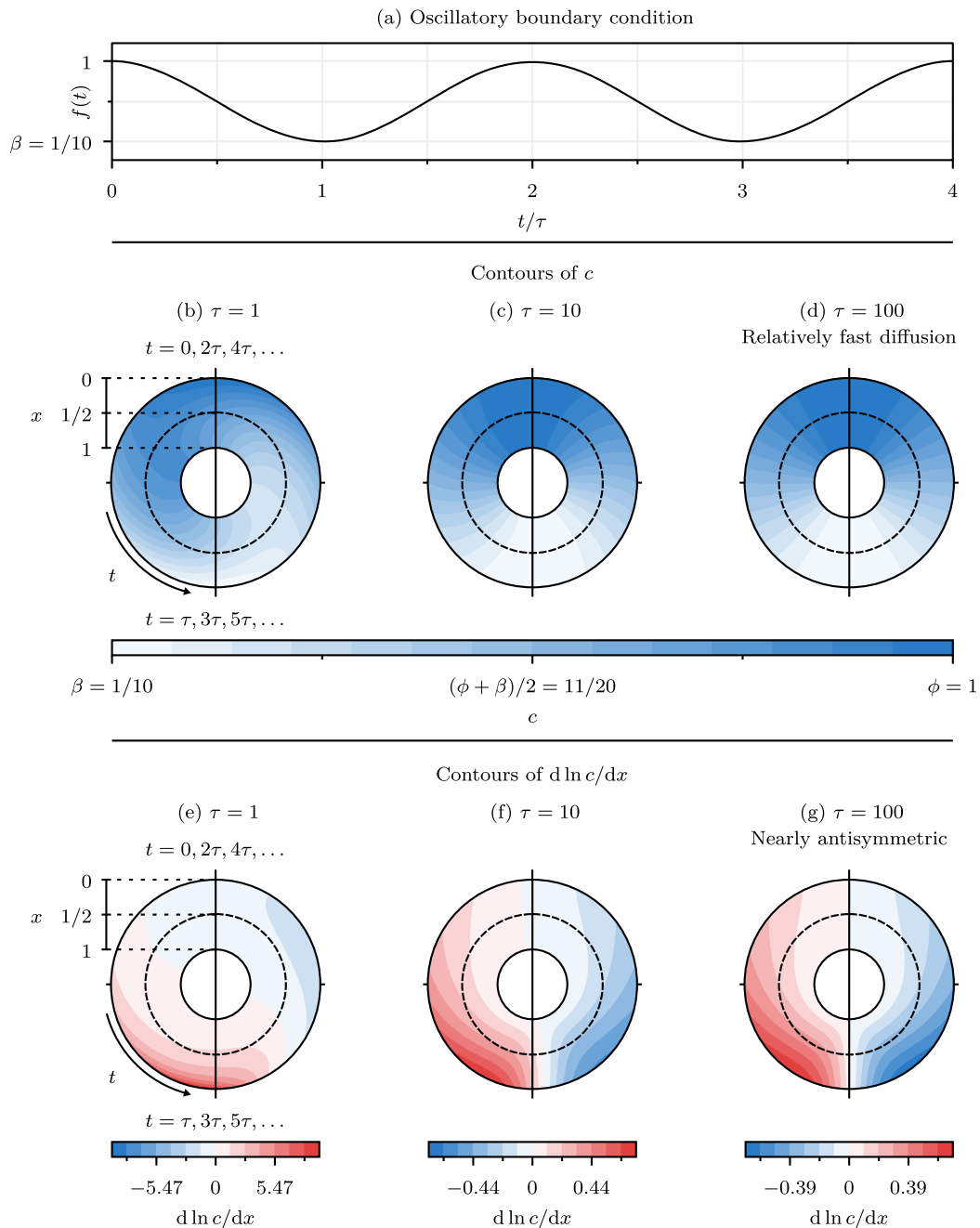
(a) Oscillatory boundary condition

Contours of c

(b) $\tau = 1$ (c) $\tau = 10$ (d) $\tau = 100$
Relatively fast diffusion

$t = 0, 2\tau, 4\tau, \ldots$

$t = \tau, 3\tau, 5\tau, \ldots$

$\beta = 1/10$ $(\phi + \beta)/2 = 11/20$ $\phi = 1$

c

Contours of $\mathrm{d}\ln c/\mathrm{d}x$

(e) $\tau = 1$ (f) $\tau = 10$ (g) $\tau = 100$
Nearly antisymmetric

$t = 0, 2\tau, 4\tau, \ldots$

$t = \tau, 3\tau, 5\tau, \ldots$

$-5.47 \quad 0 \quad 5.47$ $-0.44 \quad 0 \quad 0.44$ $-0.39 \quad 0 \quad 0.39$
$\mathrm{d}\ln c/\mathrm{d}x$ $\mathrm{d}\ln c/\mathrm{d}x$ $\mathrm{d}\ln c/\mathrm{d}x$

FIG. 5. Demonstration of linearity for a cyclical process, shown in (a), over long times. We fix the period of oscillation, 2τ, and assume that the effect of the initial condition on the concentration profile is negligible. We show contours of c in (b), (c), and (d) and contours of $d\ln c/dx$ in (e), (f), and (g). When the oscillatory timescale is comparable to the solute diffusion timescale, shown in (b) and (e) with $\tau = 1$, there is considerable asymmetry about the vertical line through integer multiples of τ. As τ increases—shown with $\tau = 10$ and 100 in (c), (d), (f), and (g)—the contours of $d\ln c/dx$ approach a configuration that is antisymmetric about the vertical line. When integrating particle trajectories with $\tau \gg 1$, the migration over either the injection or withdrawal process is negated by migration over the complementary process.

on the particle concentration in the adjoining channel, and the effect of the initial condition must be considered for real-world applications. Another important qualifier is that the notion of reversibility applies only to the particles that remain in the pore throughout the process. This result, however, still provides insight into potential applications: In an enhanced oil recovery process, for instance, slow oscillation is unlikely to confer a significant benefit to withdrawal efficiency, as oil remaining in a pore after one cycle will simply move back and forth without exiting the pore in subsequent cycles (subject to our initial assumptions about, for instance, negligible diffusion and convection at the pore inlet).

B. Fast oscillation

We turn now to cases where the oscillation in solute concentration at $x = 0$ is fast relative to solute diffusion, which complement the cases with slow oscillation discussed in Sec. VII A. One potential application of an oscillatory boundary condition is efficiency enhancement relative to configurations with monotonic changes in solute concentration. We note that, for a given system with independent injection and withdrawal processes that occur over finite time, the efficiency of one process—depending on the solute and particle species involved—will be greater than the efficiency of the complementary process. This is consistent with our observations in Fig. 4, where the efficiency metrics of complementary injection and withdrawal processes differ. Any oscillatory system with independent injection and withdrawal steps (though not slow transitions covered in Sec. VII A) has an efficiency of 1 in the limit $t \to \infty$; each pair of injection and withdrawal processes will move particles closer to either the entrance or the end of the pore. Either the injection or the withdrawal process will dominate and net migration will occur with successive application. This is more complicated, however, for oscillatory processes for which oscillation occurs over a timescale that is comparable to or smaller than the diffusion timescale; the notion of diffusive inertia becomes increasingly relevant as the timescale of the process decreases. Indeed, the frequency of oscillation is an important consideration over shorter timescales because the injection and withdrawal processes have a significant effect on each other.

To explore the efficiency of various processes with oscillation in the boundary, we consider both a step and a sinusoid with a period of 2τ. We fix the initial solute concentration as a constant $c(x, t = 0) = 1$ and set $\beta = 1/10$ and $\mathcal{M}/\mathcal{D} = 1/4$. This is an example of an injection process, and we expect particles to move toward $x = 1$ over time. We show an example in Fig. 6, which includes sample trajectories for several different values of τ. We show the boundary conditions we consider in Fig. 6(a). In this example, it is possible to exceed the efficiency associated with a step boundary condition by oscillating for a time that is $\mathcal{O}(10)$; this is annotated in Fig. 6(b). With NaCl in the $400\,\mu$m-long pore geometry studied by Shin *et al.* [1], this is $\mathcal{O}(10\,\text{min})$ with oscillations of period $\mathcal{O}(1\,\text{min})$, which is attainable in a laboratory setting with a configuration like that shown in Fig. 1(c). Notably, while each of the oscillatory conditions in the figure has an asymptotic efficiency of 1, the frequency of oscillation affects the rate of net particle migration. In the example, relatively slow oscillation is inefficient, as faster oscillations could further exploit the nonlinearity inherent to diffusiophoresis; however, very fast oscillation results in slow propagation of particles deep in the pore because the change in solute concentration is limited by the diffusion timescale. To visualize this, it may be helpful to consider oscillation at a frequency $1/2\tau \gg 1$; in such a configuration, the solute concentration near $x = 0$ would change very rapidly and have a significant effect on the dynamics of particles near the entrance, while the concentration near $x = 1$ would hardly change and particles deeper in the pore would migrate slowly. In Fig. 6(b), this manifests as the highest efficiency occurring with an intermediate value of τ, while the efficiency of both slower and faster oscillatory processes is limited. It may be possible to further increase the rate of particle migration in Fig. 6 by *varying* the frequency of oscillation: When a particle is near $x = 0$, very fast oscillation is advantageous because sharp concentration gradients can be applied repeatedly. By contrast, slower oscillation ensures the solute concentration gradient is significant for particles deeper in the pore.
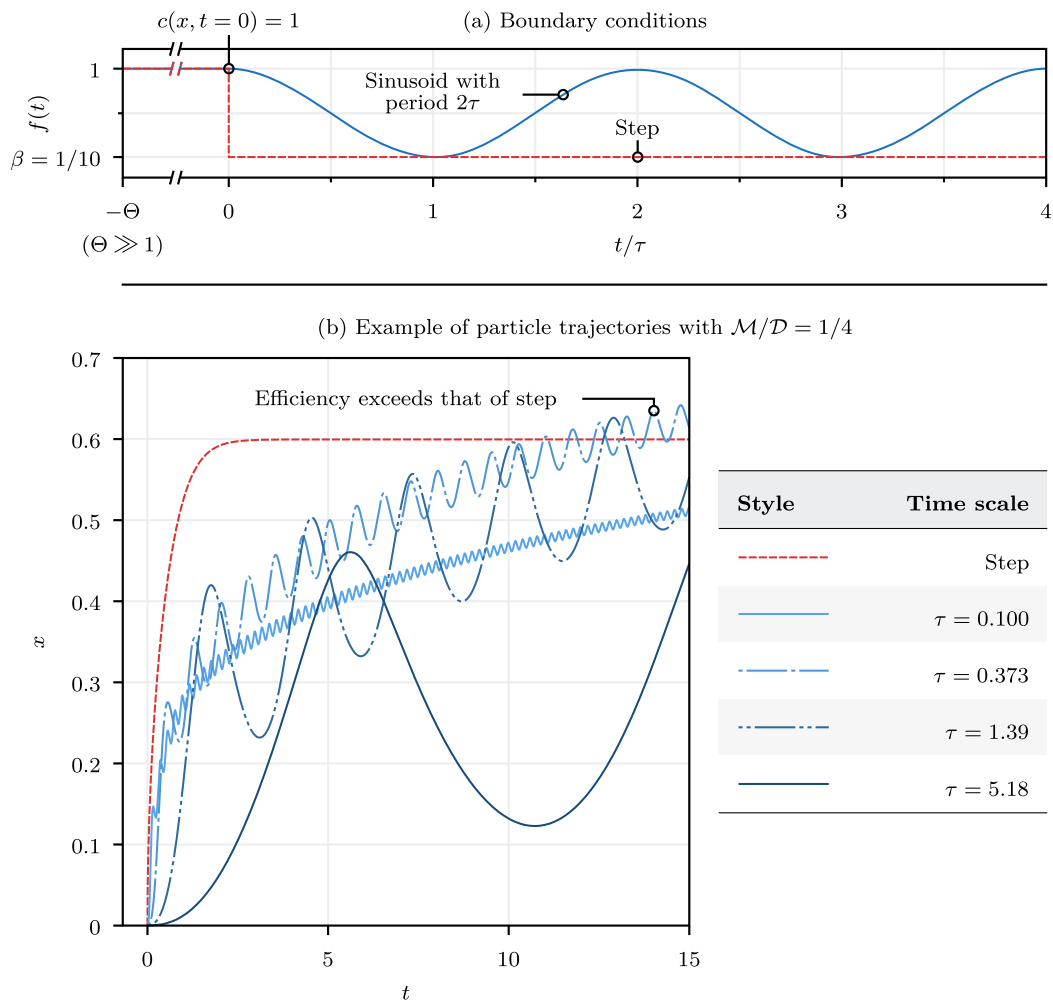
(a) Boundary conditions

$c(x, t = 0) = 1$

$f(t)$

1

$\beta = 1/10$

Sinusoid with period 2τ

Step

$-\Theta$ 0 1 2 3 4

$(\Theta \gg 1)$ t/τ

(b) Example of particle trajectories with $\mathcal{M}/\mathcal{D} = 1/4$

Efficiency exceeds that of step

Style	Time scale
– – – –	Step
——	$\tau = 0.100$
—·—·—	$\tau = 0.373$
—··—··—	$\tau = 1.39$
——	$\tau = 5.18$

FIG. 6. Demonstration of particle migration during an injection process with an oscillatory boundary. Each period of oscillation, depicted in (a), results in a net migration of particles in a fixed direction. All cases with oscillatory boundaries (except those with very slow oscillation) will eventually attain an efficiency that exceeds that associated with the step boundary condition and approaches 1 asymptotically. We demonstrate in (b) that it is likely possible to apply this to real-world systems; with $\mathcal{M}/\mathcal{D} = 1/4$ and $\beta = 1/10$, the efficiency associated with a sinusoidal boundary can exceed the efficiency associated with a step boundary where t is $\mathcal{O}(10)$. For other boundaries with a more significant contrast between injection and withdrawal efficiencies, such as repeated step conditions, the oscillatory condition may yield a higher efficiency than a single step at even lower t. Notably, the best choice of frequency depends on the solute and particle species (through $\mathcal{M}/\mathcal{D}$), the magnitude of β, and the length of time over which oscillation occurs. In (b), the particle positions at $t = 15$ have converged to within 0.1 % relative error.

Another interesting feature of rapid oscillation is that the particle dynamics change as the frequency of oscillation increases and diffusive inertia becomes more prominent. In order to demonstrate this principle, we consider a case for which we assume the boundary solute concentration has been oscillating for a long time relative to the solute diffusion timescale. This allows us to neglect the effect of the initial solute concentration and instead focus on the effects of oscillation on particle dynamics in isolation. This may be particularly relevant to cases where the efficiency of injection or
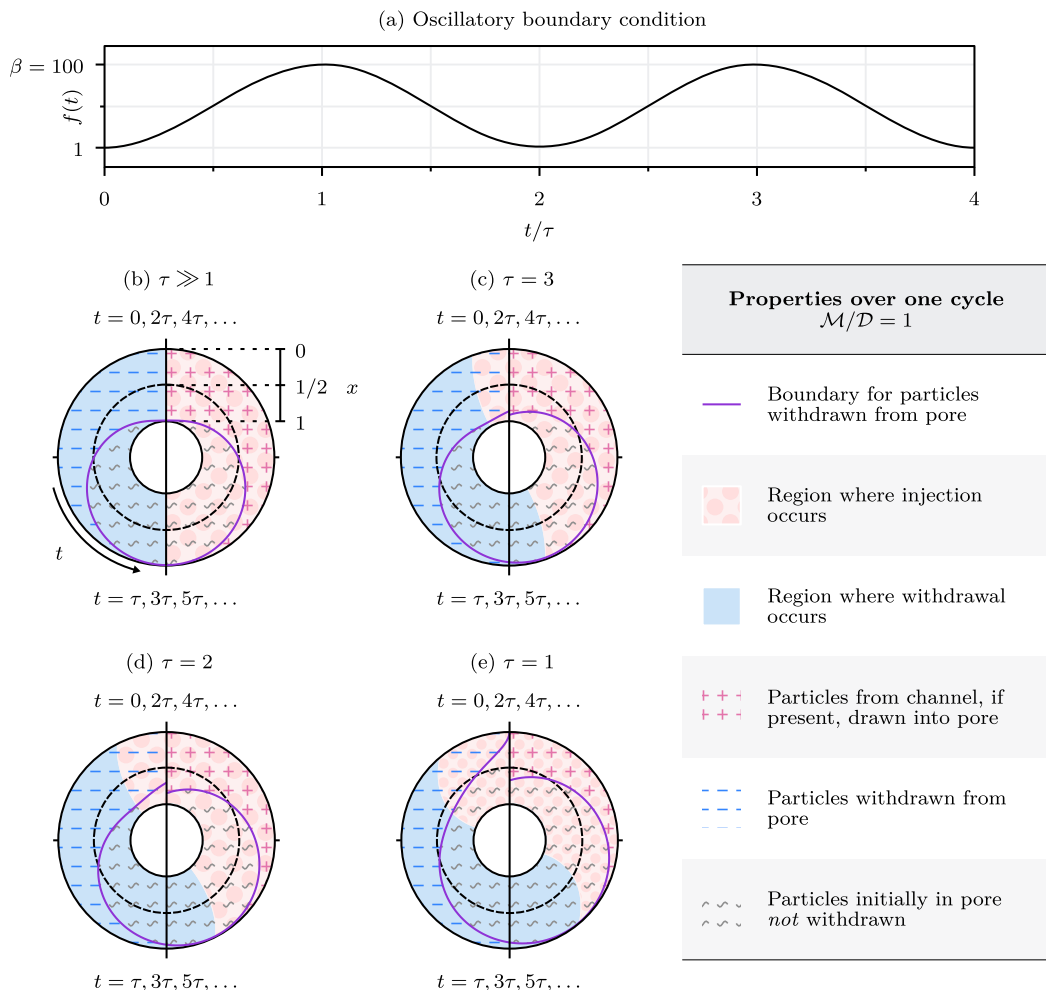
FIG. 7. Example of an oscillatory boundary condition for which the qualitative particle dynamics are dependent on the timescale of the boundary condition. We impose a sinusoidal boundary condition with a period of 2τ and an upper bound of $\beta = 100$, as shown in (a). We then consider the trajectories of particles with $\mathcal{M}/\mathcal{D} = 1$ over $t \in [n\tau, (n+2)\tau]$ for $n = 0, 2, 4, \ldots$. We assume the cycle has been occurring for long enough that the effect of the initial condition is negligible. We show regions of particle injection and withdrawal with a boundary to indicate the deepest particle that is withdrawn over one period (the particle that approaches $x = 0$ but does not reach it), calculated to within 0.1 % relative error, in (b)–(e). Plot (b) shows the case where $\tau \gg 1$, for which the particle migration is linear (see Fig. 5) and the curve defining the withdrawal boundary can be found with Eq. (8). As τ decreases, so does the degree of antisymmetry in $d \ln c/dx$ about integer multiples of τ. This causes the particle path to distort. In this case, for $\tau \approx 1$, all of the particles initially present in the pore are injected deeper over one period, as shown in (e); no particles are withdrawn. It is possible, therefore, to achieve dramatically different particle dynamics by changing only the timescale for oscillation of the solute concentration at the pore entrance.

withdrawal is relatively low, as oscillation over long times may provide a mechanism for effecting appreciable particle migration when it is otherwise unattainable over shorter timescales. We apply the sinusoidal boundary condition with a period of 2τ and a solute concentration between 1 and $\beta = 1/100$ shown in Fig. 7(a). We consider particles for which $\mathcal{M}/\mathcal{D} = 1$. The sinusoidal variation in boundary solute concentration yields withdrawal processes followed by injection processes. In

order to visualize the motion of particles, we show the trajectory of a representative particle. In Figs. 7(b)– 7(e), we show the trajectory of the particle that approaches but never crosses $x = 0$, along with regions where injection and withdrawal occur. The line indicating the particle trajectory acts as the boundary for particles that remain in the pore over one period of oscillation; any particles deeper in the pore remain there over the oscillation period, while any particles closer to the entrance are withdrawn. In Fig. 7(b), $\tau \gg 1$ and the particle trajectory is symmetric across the vertical line $t = n\tau$ for $n = 0, 1, 2, \ldots$. This is consistent with the slow-transition behavior observed in Sec. VII A. As τ decreases, the role of inertia becomes more prominent. In Fig. 7(e), which shows the case where $\tau = 1$, there is significant asymmetry across the vertical line. Notably, the region indicating particles that remain in the pore over one period of oscillation—the position of the boundary for particles at $t = 0$—changes from 1 % in Fig. 7(a), which is consistent with the efficiency defined in Eq. (10), to 100 % in Fig. 7(e).
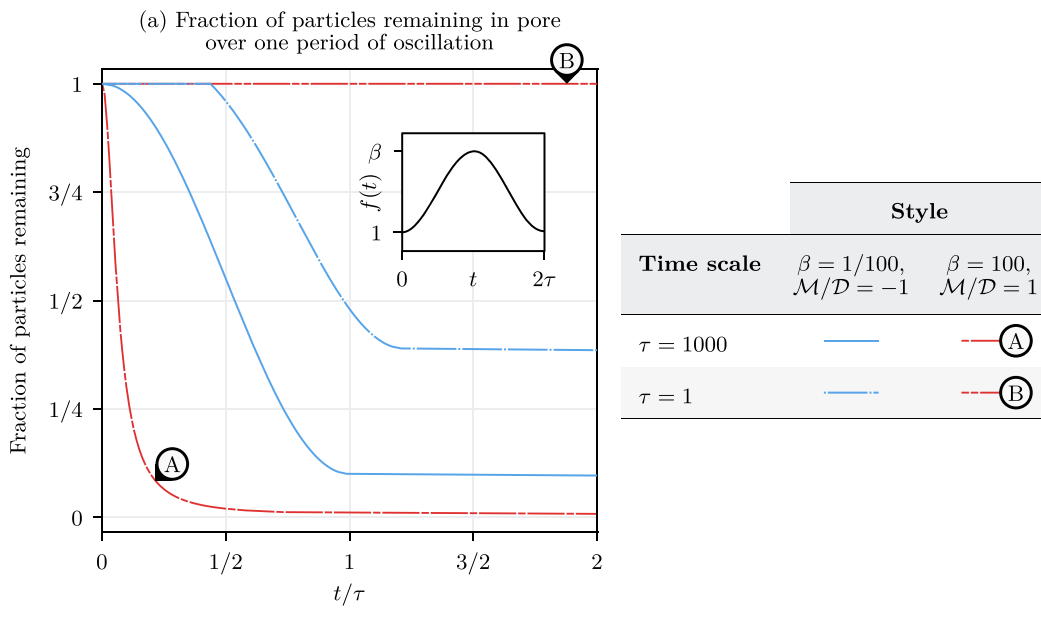
This is a dramatic change in particle dynamics. In order to examine the effects on all particles in the pore, rather than a single particle, we use a tracer field. We initialize a uniform concentration of particles when the boundary solute concentration is a minimum at $t = k\tau$ for $k = 0, 2, 4, \ldots$ to see the effects of one period of oscillation. In effect, we are assuming the concentration of particles in the pore is uniform when the boundary solute concentration is at its lowest value, then observing the motion of the particles throughout the pore. In Fig. 8(a), we show the fraction of particles remaining in the pore over time for several values of τ with an extreme solute concentration defined by $\log_{10} \beta = \pm 2$ and particles with $\mathcal{M}/\mathcal{D} = \pm 1$. Cases A and B are Figs. 7(b) and 7(e), respectively. For A ($\tau \gg 1$), most of the particles initially present in the pore are withdrawn over the first half of the period; for B ($\tau = 1$), particles are initially forced deep enough into the pore that none are withdrawn during the withdrawal phase. This is further illustrated in Fig. 8(b), which focuses on the regions where particles remain in the pore or are withdrawn in Figs. 7(b) and 7(e). This is partially the result of a phase lag—one injection or withdrawal process carries over into the next because the diffusion timescale is comparable to or larger than the oscillation timescale—but differences between the particle dynamics with fast and slow oscillation persist regardless of the phase; the trajectory in Fig. 7(e) is asymmetric even if there is a phase offset. The degree of asymmetry increases as the frequency of oscillation increases. The cases for which $\beta = 1/100$ and $\mathcal{M}/\mathcal{D} = -1$ show, qualitatively, the opposite behavior, with differences caused by the nonlinearity of the processes (the magnitude of the solute concentration).

The examples in Figs. 6 and 7 address, in part, Q4. We demonstrate in Fig. 6 that oscillation in the solute concentration at the boundary can yield an enhanced efficiency relative to a step boundary condition. Further, the asymmetry in Fig. 7 shows that the frequency of oscillation has an effect on the dynamics of particles, with the degree of asymmetry in particle trajectories increasing with oscillation frequency. This could be used to tune the frequency for specific applications; while changing the oscillation frequency does not necessarily change the direction of particle migration, it does affect the influence of an individual injection or withdrawal process, relative to the complementary process, on net particle migration.

VIII. DISCUSSION

We have demonstrated the relevance of the timescale for changes in solute concentration to particle migration in dead-end pores and illustrated that the timescale is also an essential consideration for oscillatory processes. The timescale dependence and the effects of an oscillatory boundary condition for the solute concentration may be significant to natural processes, where there exists a wide variety of timescales for the development of solute concentration gradients. Seasonal or diurnal events, such as changes in solute concentration driven by the melting or formation of ice, may be representative of slow changes in concentration; events such as sudden floods (p. 4689 in Ref. [22]) may yield steep concentration gradients over shorter timescales.

Extending our results to porous media, rather than an individual dead-end pore, may also improve our understanding of diffusiophoresis in nature and in industrial applications. While the dead-end

(a) Fraction of particles remaining in pore over one period of oscillation

	Style	
Time scale	$\beta = 1/100,$ $\mathcal{M}/\mathcal{D} = -1$	$\beta = 100,$ $\mathcal{M}/\mathcal{D} = 1$
$\tau = 1000$	——	——Ⓐ
$\tau = 1$	–·–·–	– – –Ⓑ

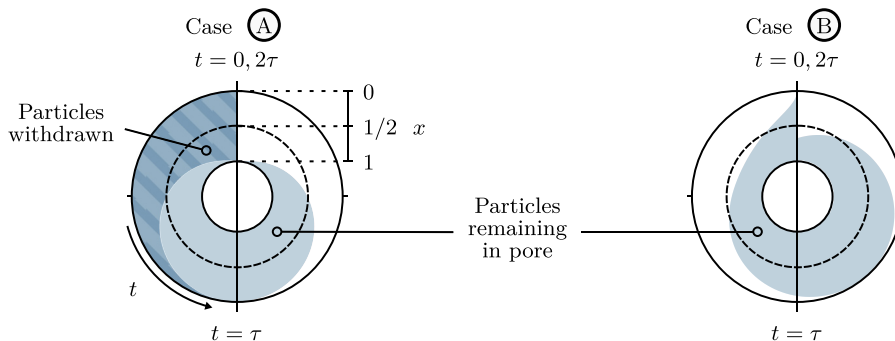(b) Depiction of regions where particles are withdrawn or injected, as in Fig. 7

FIG. 8. Demonstration of frequency dependence of injection and withdrawal processes; this figure complements Fig. 7. In (a), the fraction of particles remaining in the pore over time is shown for two values of τ and two values of β and $\mathcal{M}/\mathcal{D}$. In (b), the regions of injection and withdrawal are shown. With slow oscillation, particle withdrawal is preferred; this is depicted for $\tau = 1000$ in (a) and (b) with marker A. With rapid oscillation, particle injection is preferred; we show this with marker B. Notably, the withdrawal performance depends on β and $\mathcal{M}/\mathcal{D}$. The fraction of particles remaining in the pore is accurate to within ± 0.005.

pore is commonly used for experimental studies of diffusiophoresis, porous media with more complex geometries are likely a better representation of systems where diffusiophoresis may be relevant and are the subject of recent work by Sambamoorthy and Chu [23]. Such a system may also be more representative of industrial applications like laundry detergency [10]. Similarly, geometries with junctions [24,25] may be a natural extension of our present work.

Our assumption that particle diffusion is negligible is likely reasonable for cases where the elapsed time is comparable to the diffusion timescale of the solute. In typical applications of diffusiophoresis, the solute species are much smaller than the particles and diffuse more rapidly. However, as the elapsed time of a process increases, the validity of the assumption of negligible particle diffusion must be reconsidered. In physical systems, the slow-transition dynamics described

by Eq. (9) are likely also influenced by the diffusion of particles. The efficiency associated with oscillatory boundary conditions may also change, with a likely consequence of increased withdrawal efficiency and reduced injection efficiency. We posit, for instance, that a withdrawal process yields a steep gradient in particle concentration at the front of the particle distribution, and that particles would move toward the pore entrance diffusively prior to the next step of the oscillation. For injection processes, regions of high particle concentration (in the extreme case of an injection process with efficiency 1, all particles end at $x = 1$) would experience rapid diffusion because of the steep concentration gradient formed through the focusing of particles (p. 258 in Ref. [1]). Such considerations are outside of the scope of this work but may be of interest in future studies, particularly where theoretical and experimental results are compared. Similarly, we have neglected convection near the pore inlet, but Akdeniz *et al.* [26] recently found that "the convective flow is an essential parameter in particle dynamic behavior" in a dead-end pore when the three-dimensional dynamics are considered, which warrants further study.

Another assumption that warrants further consideration in future work is the assumption of constant diffusiophoretic mobility. It can vary with local conditions such as the temperature, pH, and solute concentration [27]. The dependence on solute concentration is particularly relevant to our work, and it may be possible to obtain distinct dynamics—such as a reversal of migration direction or an enhanced migration efficiency—with an informed choice of extreme solute concentrations. Indeed, we expect there is a solute concentration at which the diffusiophoretic mobility is maximized [28], and the particle velocity diminishes at higher or lower concentrations. Akdeniz *et al.* [26] found that a solute concentration-dependent zeta potential affects particle dynamics in dead-end pores, particularly over long timescales. Variable-mobility models may be particularly interesting, then, in the context of slow transitions or oscillatory changes in solute concentration. Variation in mobility driven by gradients in pH is another potential mechanism for controlling the particle transport rate [12]. With a strategy for modulating the diffusiophoretic mobility, we imagine that it may be possible to design systems that favor either injection or withdrawal and increase the difference between the efficiency metrics of complementary processes; oscillation *paired with* a strategy for modulating diffusiophoretic mobility could be a powerful tool for changing particle dynamics. This would complicate the problem mathematically, however, and we leave it as the subject of future work.

To make our analysis tractable, we have considered one-dimensional pores. In doing so, we have neglected all interactions occurring at channel walls. In reality, many microfluidic devices are composed of materials with a nonzero surface charge [12,28], for which diffusioosmosis is an important consideration. Explorations of fluid, solute, and particle dynamics in two- or three-dimensional geometries could yield further insights about real-world systems. Indeed, revisiting the solute concentration boundary condition with relaxed assumptions would provide further insight into real-world applications of diffusiophoresis in porous geometries, both in the laboratory and in nature.

IX. CONCLUSION

We have examined, by addressing a series of related questions (Q1–Q4), the role of the solute concentration boundary condition on the dynamics of particles within a dead-end pore. We first defined metrics for the efficiency of injection and withdrawal processes and subsequently used them to characterize the performance of systems with a steplike change in solute concentration at the boundary. Notably, differences in efficiency are a result of the nonlinearity inherent to diffusiophoresis, and the efficiency of a process depends on whether the concentration at the boundary increases or decreases relative to the initial concentration, among other things. We examined cases where the solute concentration at the boundary changes linearly over a period of time and found that the efficiency metrics of injection and withdrawal processes converge when the concentration changes slowly relative to the diffusion timescale of the solute. The diffusiophoretic migration of particles becomes linear in the slow-transition limit. This has significant implications for oscillatory

boundary conditions, as particles within a pore will simply move back and forth without a preferred direction when the solute concentration oscillates slowly. By contrast, when the period of oscillation is comparable to or less than the timescale for solute diffusion, the nonlinearity is significant and a preferred direction for particle migration is apparent. Such findings have potential applications both in the laboratory, where they could be applied to tune application-specific particle dynamics, and in nature, where there are varied timescales over which the solute concentration at a pore inlet might change. Our results also yield new questions—left to future work—about the influence and potential applications of variable-diffusiophoretic mobility models and the influence of three-dimensional effects, including convection at the pore inlet and diffusioosmosis along channel walls, on the dynamics of particles in pores with time-variable boundary solute concentration.

ACKNOWLEDGMENT

APPENDIX: SOLUTIONS FOR SOLUTE CONCENTRATION PROFILES

We present several methods for modeling the solute concentration profile. These allow us to evaluate the solute concentration at individual points in time and space, and to integrate particle trajectories backward in time without using a significant amount of memory (numerical solutions, by contrast, would require us to save the solution everywhere in the domain because the diffusion equation is not time reversible). We are modeling the dynamics of solute and particles as a result of changes in the boundary concentration $f(t)$. Determining the concentration at any position x and time t is therefore essential to our models, and we seek cases where the solution to the governing equation, Eq. (6), can be simplified. We note the presence of f' in an integral over time. This suggests the solution may be considerably simplified in several cases. First, we note that cases with a step boundary simplify considerably (Appendix 1); the solution has been used in other works [1]. Another case where a significant simplication is possible is when f is linear, such that f' is constant. Such a condition also applies to functions composed of a finite number of linear segments (Appendix 2): the derivative in such cases remains integrable because the number of discontinuities is countable and individual points have no effect on the integral. We let $\xi = \pi(2a - 1)$ and $\gamma = -\pi^2(2a - 1)^2/4 = -\xi^2/4$ to simplify notation throughout.

1. Solution for a step boundary

We determine the solute concentration by solving Eq. (6) with a step boundary condition, where the concentration at the boundary changes from $f(t = 0) = 1$ to $f(t = \tau) = \beta$. This is

$$f(t) = (\beta - 1)\mathcal{H}(t - \tau) + 1, \tag{A1}$$

where $\mathcal{H}$ is the Heaviside step function and β is the solute concentration at $t \to \infty$. The derivative, $f'(t)$, is then the Dirac delta distribution, $(\beta - 1)\delta(t - \tau)$. We evaluate the integral in Eq. (6) and find the solute concentration,

$$c(x, t) = \begin{cases} 1, & \text{if } t \leqslant \tau \\ \beta - (\beta - 1)4 \sum_{a=1}^{\infty} \frac{\sin(\xi x/2)}{\xi} e^{\gamma(t-\tau)}, & \text{if } t > \tau \end{cases}. \tag{A2}$$

This is a dimensionless version of the solution given by Shin *et al.* (see the supporting information in Ref. [1]). It can be approximated with the piecewise linear boundary condition described in Eq. (A3) by replacing the step with a large but finite slope. This may converge more rapidly because the terms in each sum in Eq. (A7) contain an additional factor of γ^{-1} (which contains a^{-2} for index a) that is not present in the sum in Eq. (A2).

2. Solution for a piecewise linear boundary

We also solve Eq. (6) for a piecewise linear boundary condition, which allows us to evaluate slower changes in the boundary concentration. We impose the boundary condition

$$
f(t) = \begin{cases} c_0 + m_0 t, & \text{if } t_0 \leqslant t < t_1 \\ c_1 + m_1 t, & \text{if } t_1 \leqslant t < t_2 \\ \dots, & \dots \\ c_q + m_q t, & \text{if } t_q \leqslant t; \end{cases} \tag{A3}
$$

the integral in Eq. (6) then becomes, for $t > t_q$,

$$
\int_{t_0}^{t} db \, \frac{e^{\gamma(t-b)} f'(b)}{\pi(2a-1)} = \int_{t_0}^{t_1} db \, \frac{e^{\gamma(t-b)} m_0}{\pi(2a-1)} + \int_{t_1}^{t_2} db \, \frac{e^{\gamma(t-b)} m_1}{\pi(2a-1)} + \dots + \int_{t_q}^{t} db \, \frac{e^{\gamma(t-b)} m_q}{\pi(2a-1)}. \tag{A4}
$$

The result is similar for times $t \leqslant t_q$; the expanded integral simply includes fewer terms. This result simplifies considerably because the only dependence on b is now within the exponential term. We integrate and simplify to rewrite Eq. (A4) as

$$
\int_{t_0}^{t} db \, \frac{e^{\gamma(t-b)} f'(b)}{\pi(2a-1)} = \frac{1}{\gamma\xi}[e^{\gamma(t-t_0)} m_0 + e^{\gamma(t-t_1)}(m_1 - m_0)
$$
$$
+ e^{\gamma(t-t_2)}(m_2 - m_1) + \dots + e^{\gamma(t-t_q)}(m_q - m_{q-1}) - m_q], \tag{A5}
$$

where all but the first and last terms follow a pattern on simplification. Therefore, the concentration can be written, for $\psi \geqslant 1$, as

$$
c(x,t) = f(t) - 4 \sum_{a=1}^{\infty} \left\{ \frac{\sin(\xi x/2)}{\gamma\xi} \left[e^{\gamma(t-t_0)} m_0 - m_\psi + \sum_{i=1}^{\psi} e^{\gamma(t-t_i)}(m_i - m_{i-1}) \right] \right\}, \tag{A6}
$$

where ψ is the interval containing t. It is the index of the current linear segment of the boundary condition, starting at 0. A similar solution will also work for $\psi = 0$; the inner sum simply vanishes in such a case because only the first line segment is required to define the concentration. The sum can be rewritten as three sums S_j (so $\sum_{j=1}^{3} S_j$ is equivalent to the sum) with

$$
S_1 = m_0 \sum_{a=1}^{\infty} \frac{\sin(\xi x/2)}{\gamma\xi} e^{\gamma(t-t_0)},
$$
$$
S_2 = -m_\psi \sum_{a=1}^{\infty} \frac{\sin(\xi x/2)}{\gamma\xi}, \quad \text{and} \tag{A7}
$$
$$
S_3 = \sum_{a=1}^{\infty} \left[\frac{\sin(\xi x/2)}{\gamma\xi} \sum_{i=1}^{\psi} e^{\gamma(t-t_i)}(m_i - m_{i-1}) \right].
$$

This simplification makes it possible to rewrite S_2 to reduce the number of terms in the sum. We note that

$$
S_2 = \frac{4m_\psi}{\pi^3} \left[\sin(\pi x/2) + \frac{1}{27}\sin(3\pi x/2) + \frac{1}{125}\sin(5\pi x/2) + \frac{1}{343}\sin(7\pi x/2) + \dots \right], \tag{A8}
$$

which we write, for $x \in [0, 1]$, as $m_\psi (x/4 - x^2/8)$. The concentration simplifies to

$$c(x, t) = f(t) + m_\psi (x^2/2 - x) - 4 \sum_{a=1}^{\infty} \left\{ \frac{\sin(\xi x/2)}{\gamma \xi} \left[e^{\gamma(t-t_0)} m_0 + \sum_{i=1}^{\psi} e^{\gamma(t-t_i)} (m_i - m_{i-1}) \right] \right\}.$$
(A9)

We can now use this result to calculate particle trajectories, as the gradient of the logarithm of the concentration appears in the expression for particle velocity; we find

$$\frac{1}{c} \frac{\partial c}{\partial x} = \frac{2m_\psi (x - 1) + \frac{16}{\pi^2} \sum\limits_{a=1}^{\infty} T_a(t)(2a - 1)^{-2} \cos(\xi x/2)}{2f(t) + m_\psi (x^2 - 2x) + \frac{32}{\pi^3} \sum\limits_{a=1}^{\infty} T_a(t)(2a - 1)^{-3} \sin(\xi x/2)},$$
(A10)

where the time dependence

$$T_a(t) = e^{\gamma(t-t_0)} m_0 + \sum_{i=1}^{\psi} e^{\gamma(t-t_i)} (m_i - m_{i-1})$$
(A11)

accounts for the history of each segment of the boundary condition. In cases where the number of boundary segments is significant, it may be possible to reduce the number of terms used to calculate $T(t)$ by performing the summation from $\psi - N$ to ψ, provided N is sufficiently large: Each term decays exponentially and the effect of boundary segments on the concentration field diminishes rapidly with time.

---

[1] S. Shin, E. Um, B. Sabass, J. T. Ault, M. Rahimi, P. B. Warren, and H. A. Stone, Size-dependent control of colloid transport via solute gradients in dead-end channels, Proc. Natl. Acad. Sci. USA **113**, 257 (2016).

[2] S. Shim, Diffusiophoresis, diffusioosmosis, and microfluidics: Surface-flow-driven phenomena in the presence of flow, Chem. Rev. **122**, 6986 (2022).

[3] S. Shin, J. T. Ault, J. Feng, P. B. Warren, and H. A. Stone, Low-cost zeta potentiometry using solute gradients, Adv. Mater. **29**, 1701516 (2017).

[4] H. J. Keh and S. B. Chen, Diffusiophoresis and electrophoresis of colloidal cylinders, Langmuir **9**, 1142 (1993).

[5] A. Kar, T.-Y. Chiang, I. O. Rivera, A. Sen, and D. Velegol, Enhanced transport into and out of dead-end pores, ACS Nano **9**, 746 (2015).

[6] S. Vrhovec Hartman, B. Božič, and J. Derganc, Migration of blood cells and phospholipid vesicles induced by concentration gradients in microcavities, New Biotechnol. **47**, 60 (2018).

[7] Q. A. E. Peter, R. P. B. Jacquat, T. W. Herling, P. K. Challa, T. Kartanas, and T. P. J. Knowles, Microscale diffusiophoresis of proteins, J. Phys. Chem. B **126**, 8913 (2022).

[8] M. Wanunu, W. Morrison, Y. Rabin, A. Y. Grosberg, and A. Meller, Electrostatic focusing of unlabelled DNA into nanoscale pores using a salt gradient, Nat. Nanotechnol. **5**, 160 (2010).

[9] B. M. Alessio, S. Shim, A. Gupta, and H. A. Stone, Diffusioosmosis-driven dispersion of colloids: A Taylor dispersion analysis with experimental validation, J. Fluid Mech. **942**, A23 (2022).

[10] S. Shin, P. B. Warren, and H. A. Stone, Cleaning by surfactant gradients: Particulate removal from porous materials and the significance of rinsing in laundry detergency, Phys. Rev. Appl. **9**, 034012 (2018).

[11] B. M. Alessio, S. Shim, E. Mintah, A. Gupta, and H. A. Stone, Diffusiophoresis and diffusioosmosis in tandem: Two-dimensional particle motion in the presence of multiple electrolytes, Phys. Rev. Fluids **6**, 054201 (2021).

[12] S. Shim, J. K. Nunes, G. Chen, and H. A. Stone, Diffusiophoresis in the presence of a pH gradient, Phys. Rev. Fluids **7**, 110513 (2022).

[13] S. Battat, J. T. Ault, S. Shin, S. Khodaparast, and H. A. Stone, Particle entrainment in dead-end pores by diffusiophoresis, Soft Matter **15**, 3879 (2019).

[14] M. Nooryani, A. M. Benneker, and G. Natale, Self-generated exclusion zone in a dead-end pore microfluidic channel, Lab Chip **23**, 2122 (2023).

[15] J. T. Ault, P. B. Warren, S. Shin, and H. A. Stone, Diffusiophoresis in one-dimensional solute gradients, Soft Matter **13**, 9015 (2017).

[16] J. L. Wilson, S. Shim, Y. E. Yu, A. Gupta, and H. A. Stone, Diffusiophoresis in multivalent electrolytes, Langmuir **36**, 7014 (2020).

[17] A. Gupta, S. Shim, L. Issah, C. McKenzie, and H. A. Stone, Diffusion of multiple electrolytes cannot be treated independently: Model predictions with experimental validation, Soft Matter **15**, 9965 (2019).

[18] T.-Y. Chiang and D. Velegol, Multi-ion diffusiophoresis, J. Colloid Interface Sci. **424**, 120 (2014).

[19] J. Palacci, C. Cottin-Bizonne, C. Ybert, and L. Bocquet, Osmotic traps for colloids and macromolecules based on logarithmic sensing in salt taxis, Soft Matter **8**, 980 (2012).

[20] H. J. Keh, Diffusiophoresis of charged particles and diffusioosmosis of electrolyte solutions, Curr. Opin. Colloid Interface Sci. **24**, 13 (2016).

[21] Fick's first law of diffusion requires $dc/dx = 0$ at $x = 1$ to satisfy the no-flux condition in the absence of flow.

[22] D. Velegol, A. Garg, R. Guha, A. Kar, and M. Kumar, Origins of concentration gradients for diffusiophoresis, Soft Matter **12**, 4686 (2016).

[23] S. Sambamoorthy and H. C. W. Chu, Diffusiophoresis of a spherical particle in porous media, Soft Matter **19**, 1131 (2023).

[24] S. Shin, J. T. Ault, P. B. Warren, and H. A. Stone, Accumulation of colloidal particles in flow junctions induced by fluid flow and diffusiophoresis, Phys. Rev. X **7**, 041038 (2017).

[25] J. T. Ault, S. Shin, and H. A. Stone, Characterization of surface–solute interactions by diffusioosmosis, Soft Matter **15**, 1582 (2019).

[26] B. Akdeniz, J. A. Wood, and R. G. H. Lammertink, Diffusiophoresis and diffusio-osmosis into a dead-end channel: Role of theconcentration-dependence of zeta potential, Langmuir **39**, 2322 (2023).

[27] B. J. Kirby and E. F. Hasselbrink Jr., Zeta potential of microfluidic substrates: 2. Data for polymers, Electrophoresis **25**, 203 (2004).

[28] R. E. Migacz, G. Durey, and J. T. Ault, Convection rolls and three-dimensional particle dynamics in merging solute streams, Phys. Rev. Fluids **8**, 114201 (2023).